The importance of shear in the *bcc* → *hcp* transformation in iron

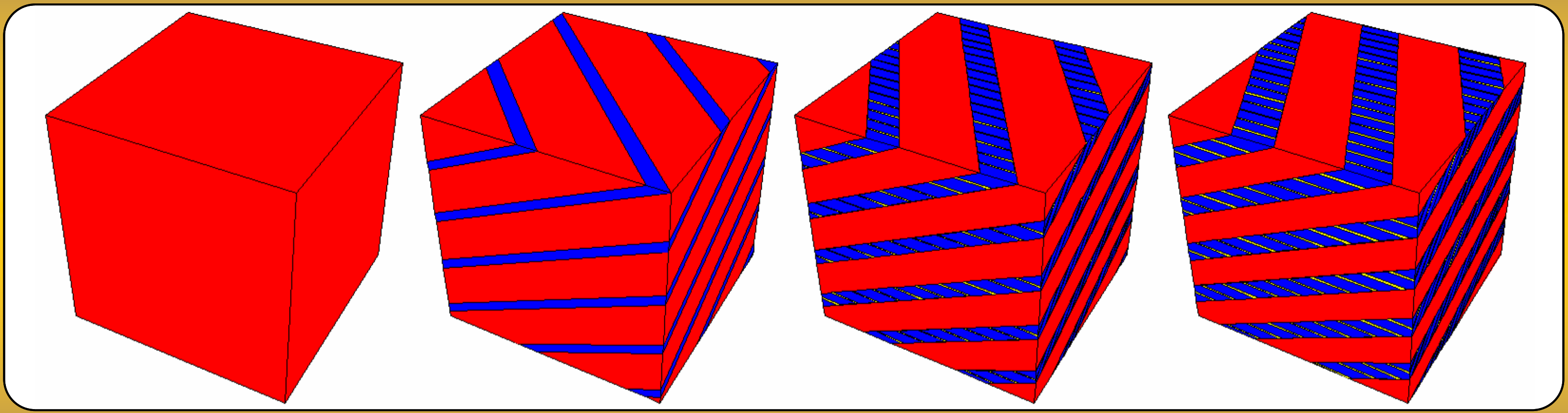

Kyle J. Caspersen and Emily Carter
Department of Chemistry and Biochemistry
University of California Los Angeles

Adrian Lew* and Michael Ortiz
Graduate School of Aeronautics
California Institute of Technology

Funded by the Department of Energy - Accelerated Strategic Computing Initiative (DOE-ASCI)

*Stanford University

Phase transformations in iron

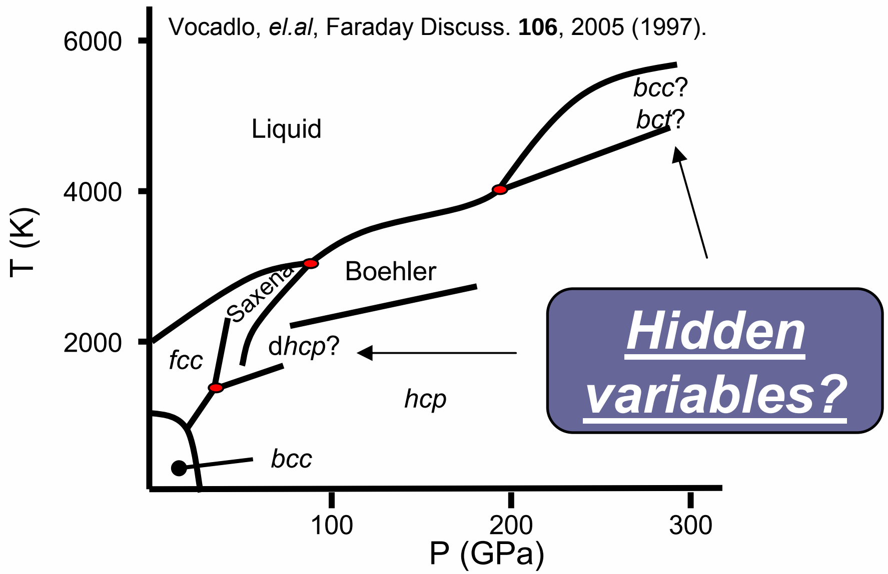

A strong shock wave will induce phase transitions producing complicated microstructure.

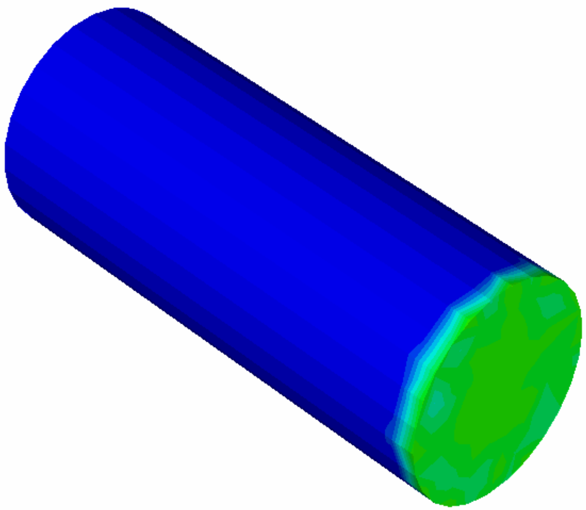

Ground state ferromagnetic *bcc* undergoes a *martensitic* phase transformation to non-magnetic *hcp* at ~10 GPa.

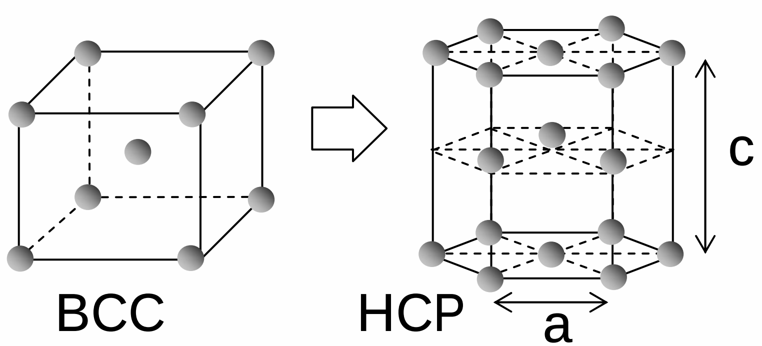

- Large scatter in the measured TP
- Fuzzy phase boundaries
- Mixed states
- Large hysteresis

Goal: understand scatter and hysteresis in transition pressures

Phase transformations in iron

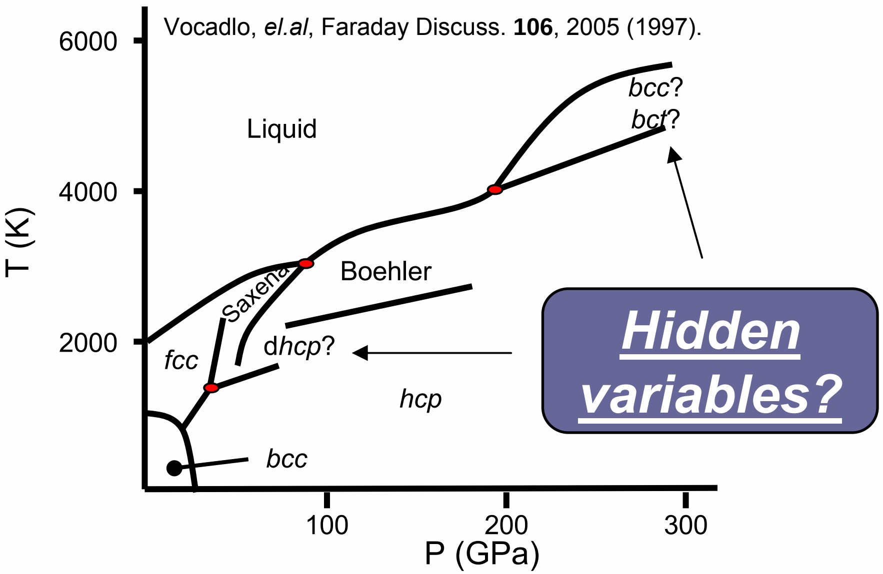

A strong shock wave will induce phase transitions producing complicated microstructure.

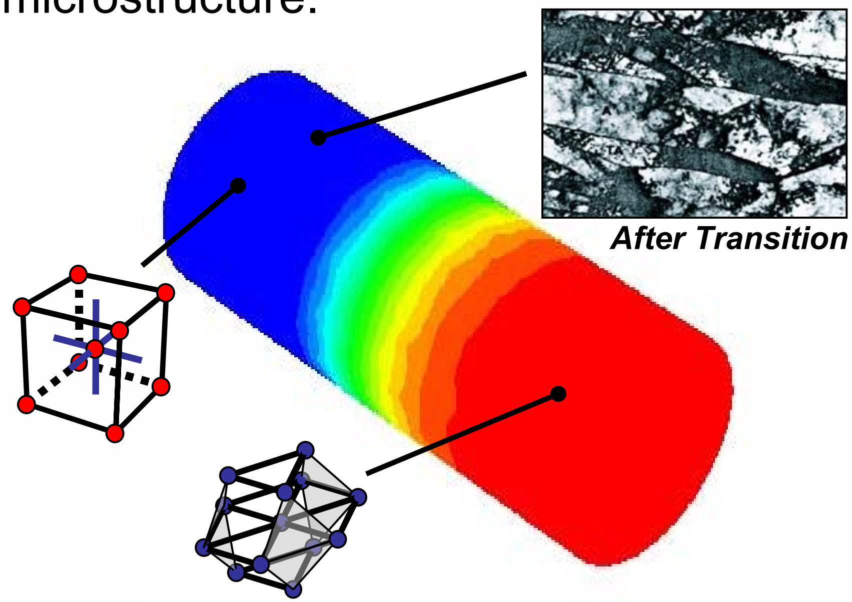

Ground state ferromagnetic *bcc* undergoes a *martensitic* phase transformation to non-magnetic *hcp* at ~10 GPa.

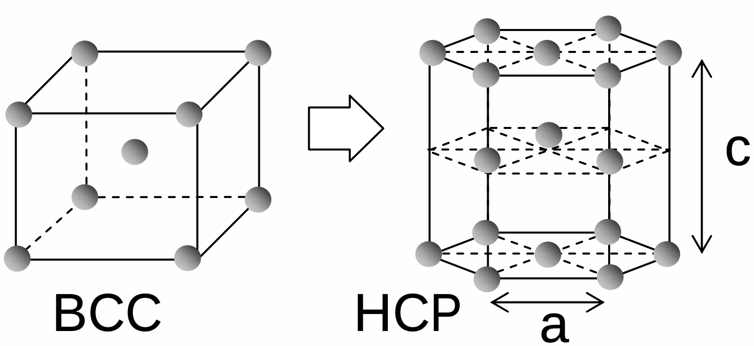

- Large scatter in the measured TP
- Fuzzy phase boundaries
- Mixed states
- Large hysteresis

Goal: understand scatter and hysteresis in transition pressures

Martensite in iron – length scales

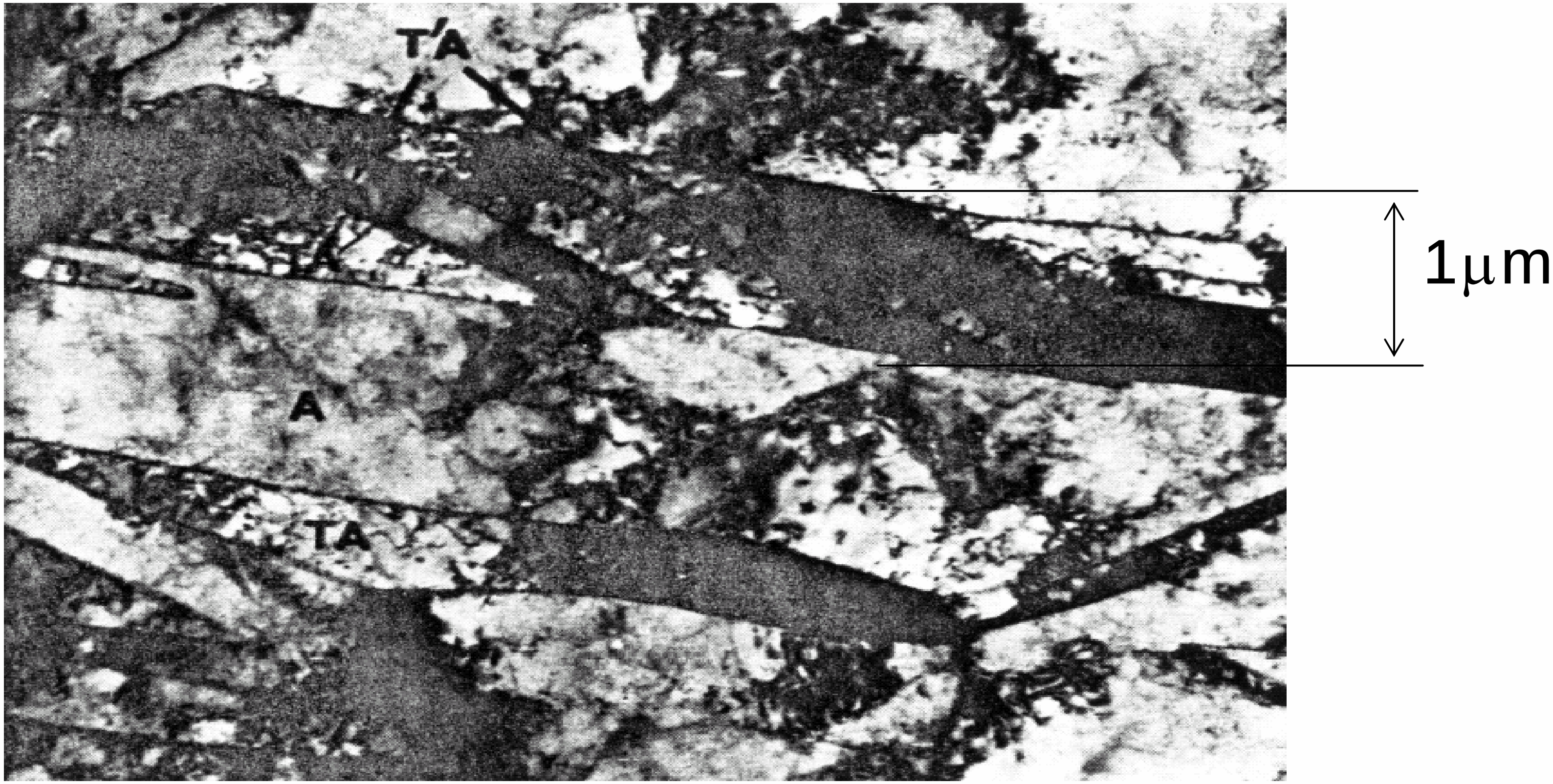

• Variants of bcc Fe produced by bcc→hcp→bcc transformation induced by shock loading (Bowden and Kelly)
• Micron-length scales require continuum analysis!

Atomistic – continuum connexion

Cauchy-Born Rule

undeformed

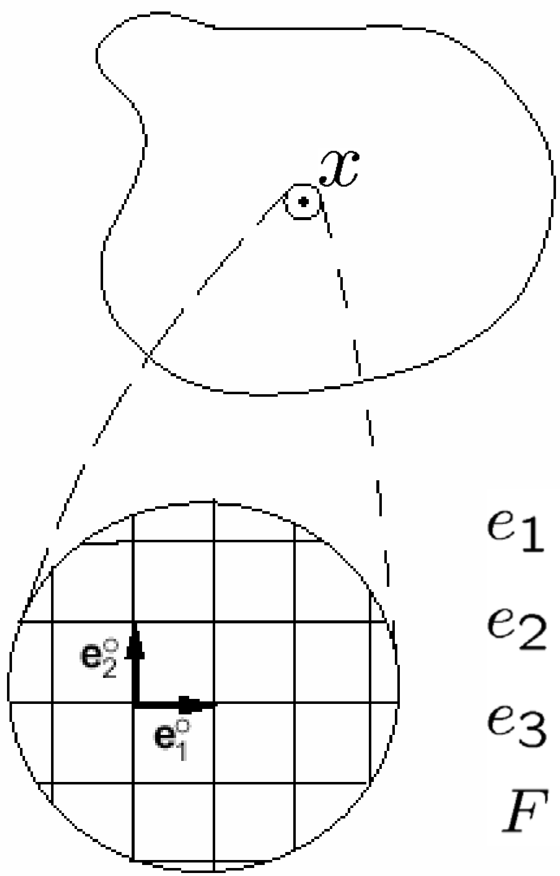

deformed

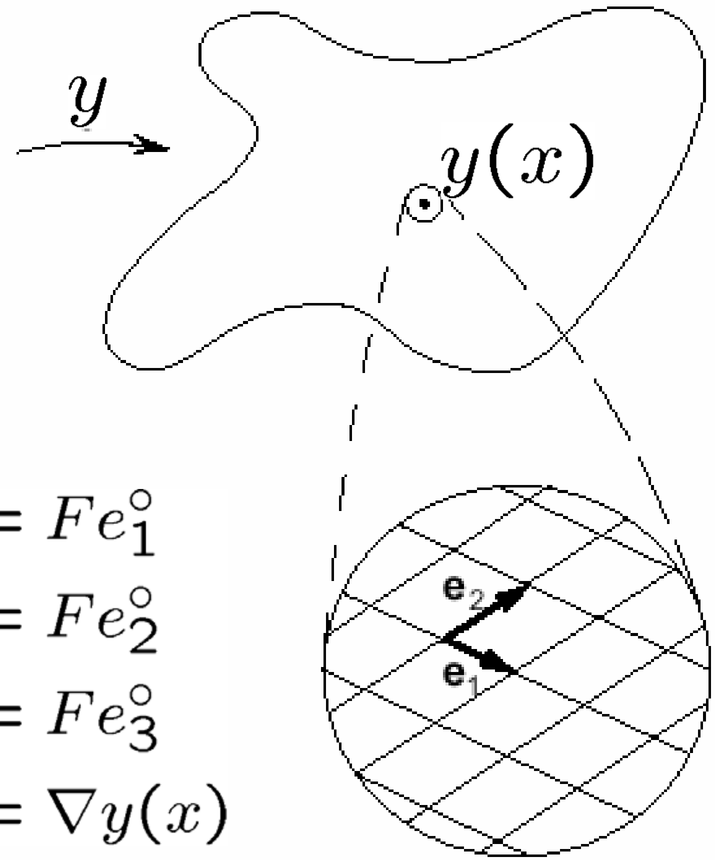

$$e_1 = F e_1^\circ$$
$$e_2 = F e_2^\circ$$
$$e_3 = F e_3^\circ$$
$$F = \nabla y(x)$$

Kinematics of *bcc*→*hcp*→*bcc* phase transformations

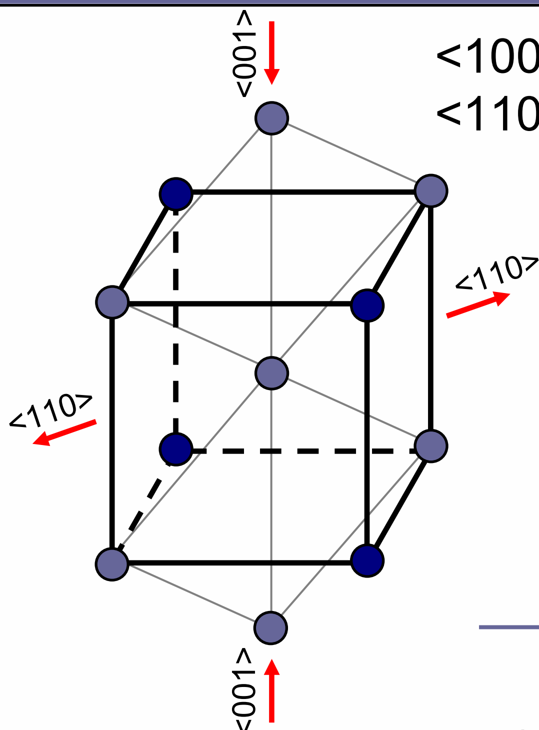

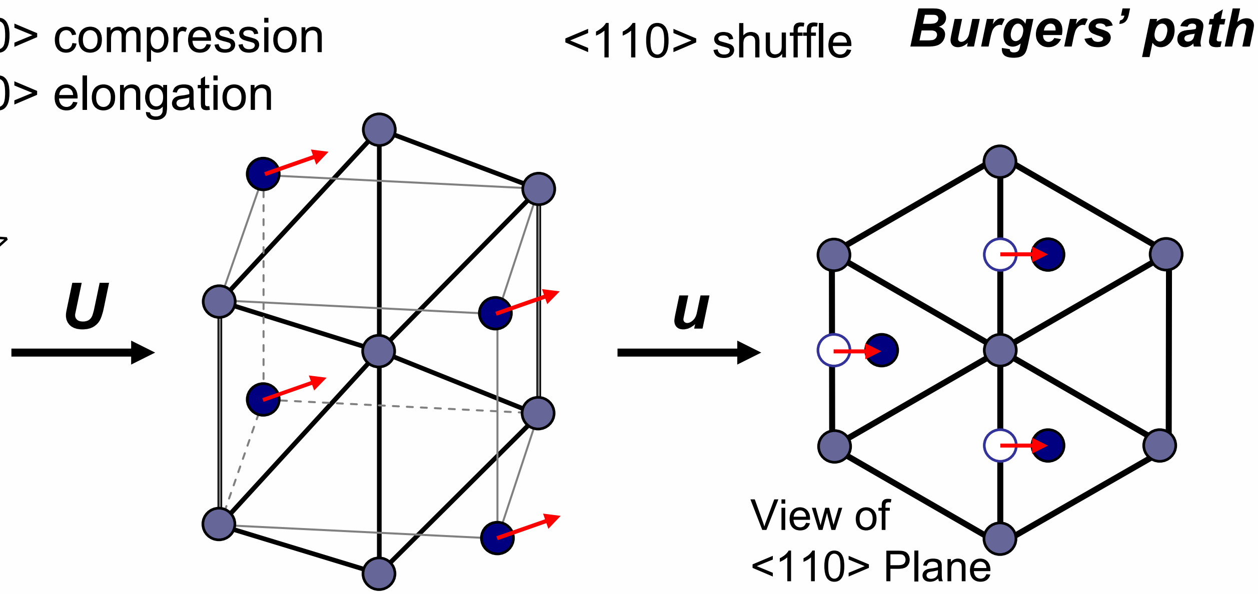

Burgers' path

$$\boldsymbol{U}(V) = \begin{pmatrix} \frac{\alpha(V)}{2} + \frac{3}{4\sqrt{2}} & \frac{\alpha(V)}{2} - \frac{3}{4\sqrt{2}} & 0 \\ \frac{\alpha(V)}{2} - \frac{3}{4\sqrt{2}} & \frac{\alpha(V)}{2} + \frac{3}{4\sqrt{2}} & 0 \\ 0 & 0 & \frac{\sqrt{3}}{2} \end{pmatrix} \qquad \boldsymbol{u} = \begin{pmatrix} \frac{1}{4\sqrt{2}} \\ \frac{-1}{4\sqrt{2}} \\ 0 \end{pmatrix}$$

- ***U*** is an *hcp* deformation
- ***u*** is the shuffle
- $\alpha(V) = \sqrt{3/8}\,(c/a)_V$

initial *bcc* variant		6 *hcp* variants		12 *bcc* variants
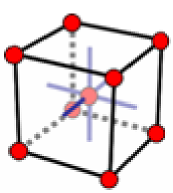	***UG*** →	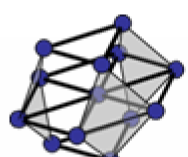	***G^{-1}U^{-1}HUG*** →	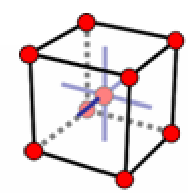
G∈ *bcc* point group		***H***∈ *hcp* point group		19 total variants

Multi-well elastic energy for iron

$$W(\boldsymbol{F}) = \min_{i=0,\dots,18} W^i(\boldsymbol{F})$$

DFT calculations prove to costly for on-the-fly W(*F*) or tabulated W(*F*)

Assumption: each deformation close to deformation of a variant

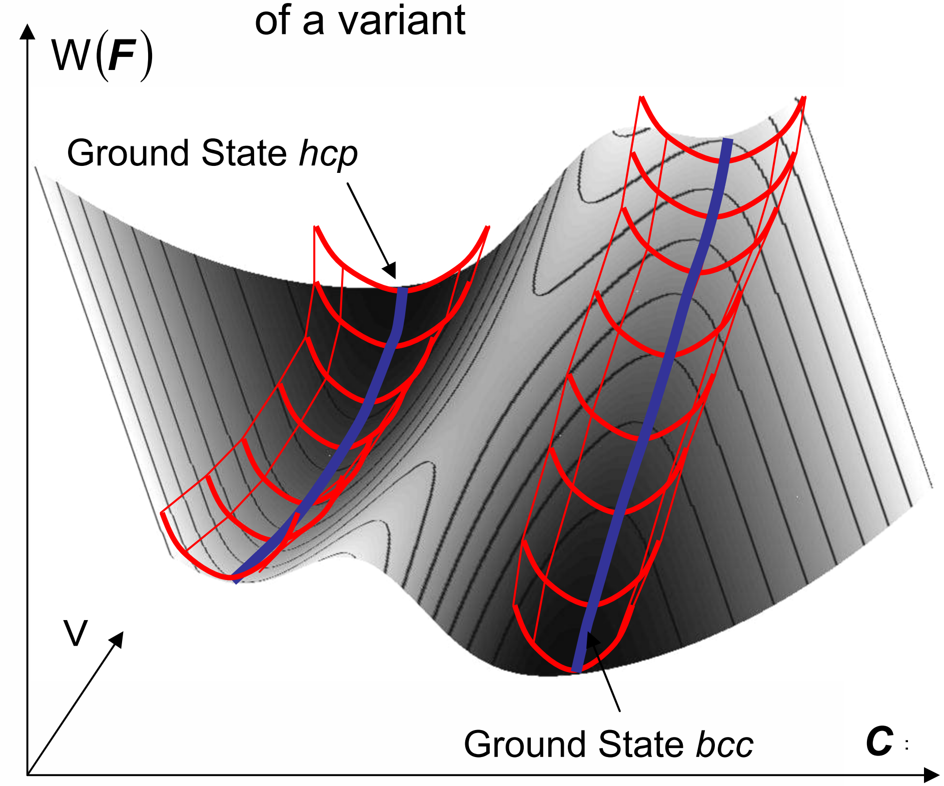

Approximation: Taylor expansion around variant deformation

Taylor Expansion

$$W^i(\boldsymbol{C}) = W^i_0(V) + \tfrac{1}{2}\left(\boldsymbol{C} - \boldsymbol{C}^i(V)\right)^T \boldsymbol{\Gamma}^i(V)\left(\boldsymbol{C} - \boldsymbol{C}^i(V)\right)$$

$$\boldsymbol{\Gamma}^i(V) = \left.\frac{\partial^2 W^i}{\partial \boldsymbol{C}^2}\right|_{\boldsymbol{C}^i(V)} \qquad \boldsymbol{C} = \boldsymbol{F}^T\boldsymbol{F}$$

DFT Calculations

- Variant deformation, $\boldsymbol{C}^i(V)$ (*hcp* c/a ratio)
- Equation of State, $W^i_0(V) = W^i(\boldsymbol{C}^i(V))$
- Non-Linear Elastic Constants, $\boldsymbol{\Gamma}^i(V)$ (Calculated using volume conserving shears)

bcc and *fcc* : $\Gamma_{11}\ \Gamma_{12}\ \Gamma_{44}$

hcp : $\Gamma_{11}\ \Gamma_{33}\ \Gamma_{12}\ \Gamma_{13}\ \Gamma_{44}$

DFT Details

- Kohn-Sham DFT within VASP
- GGA and PW-91
- Projector Augmented Wave (PAW) all electron method
- 2 Ions/Cell
- 24×24 ×24 Monkhorst Pack K-Point Grid
- 500 eV Kinetic Energy Cut Off
- Spin-Polarized for *bcc*

First-principles input into continuum model

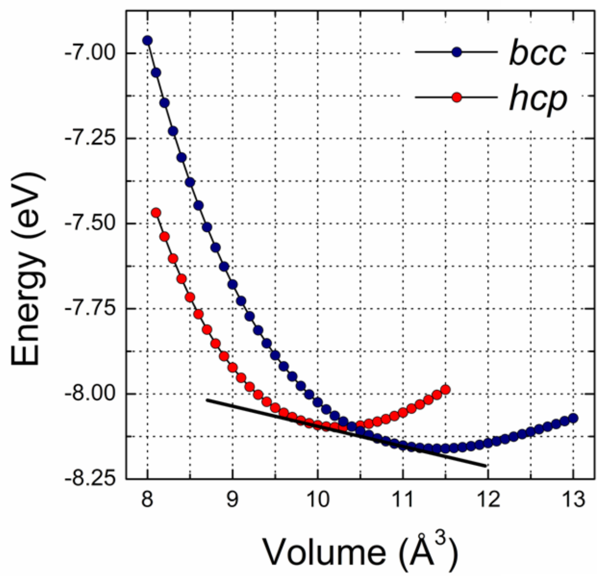

$bcc \rightarrow hcp$	Transition Pressure (GPa)
EXPERIMENT	10-15
FLAPW*	11.5
PAW	10

- PAW predicts the *bcc* to *hcp* transition pressure within the measured range

* Herper, et.al, Phys. Rev. B **60**, 3839 (1999).

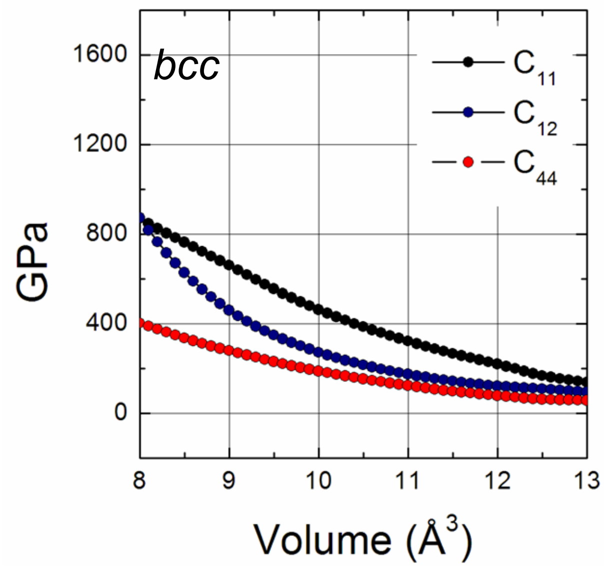

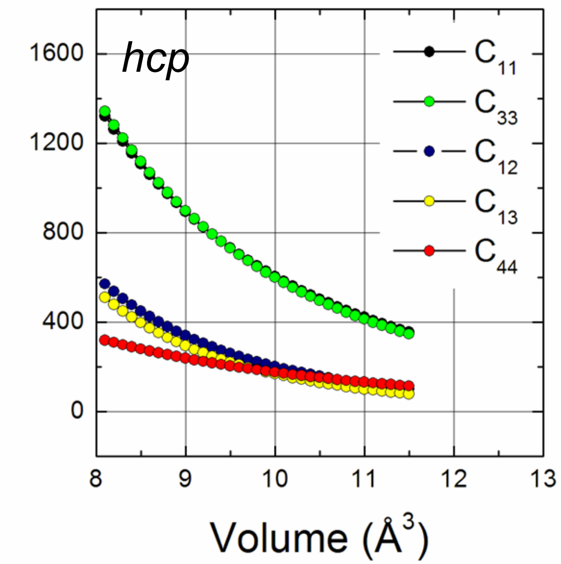

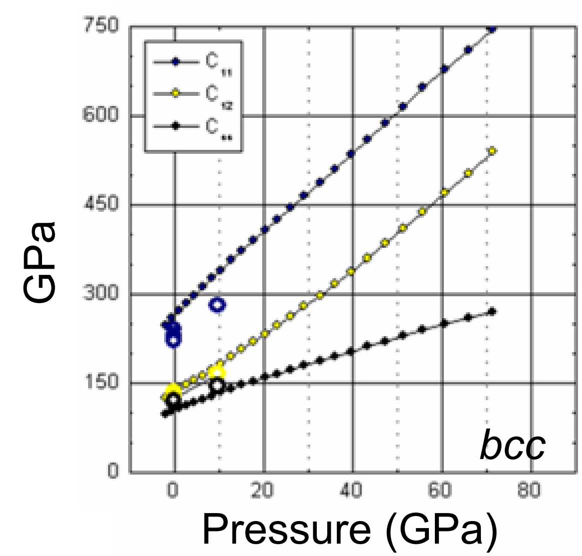

- *bcc* elastic constants compare well with experiment (C_{11} a bit high)
- little experimental data for *hcp*

Multi-well elastic energy → phase mixing!

Multi-well free-energy density with 19 variants:

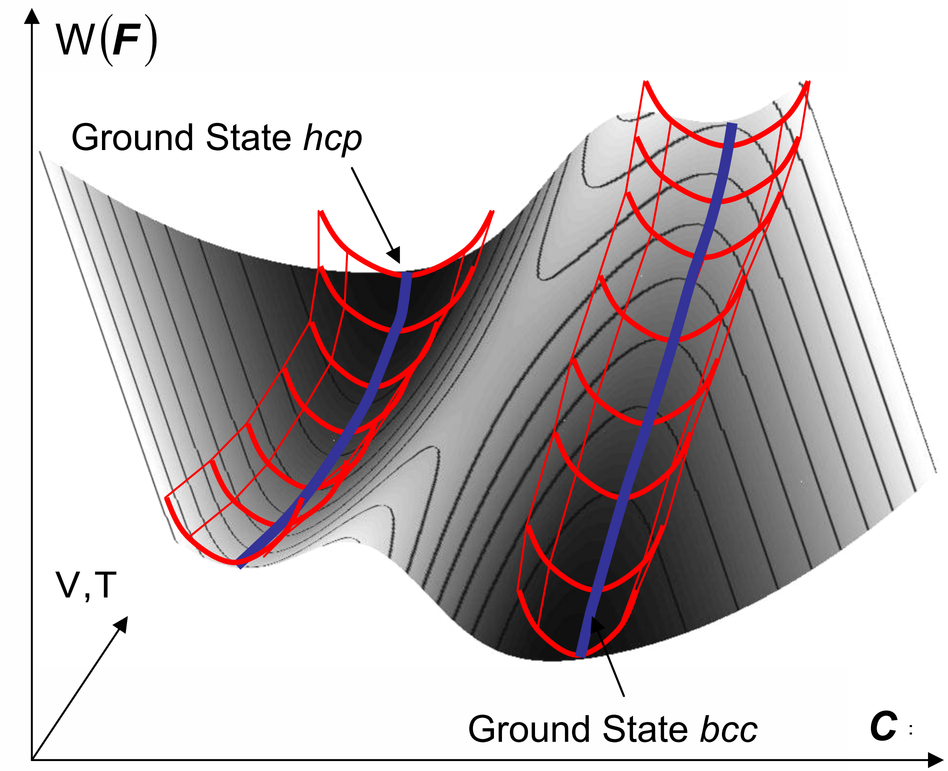

Approximation: Taylor expansion around variant deformation

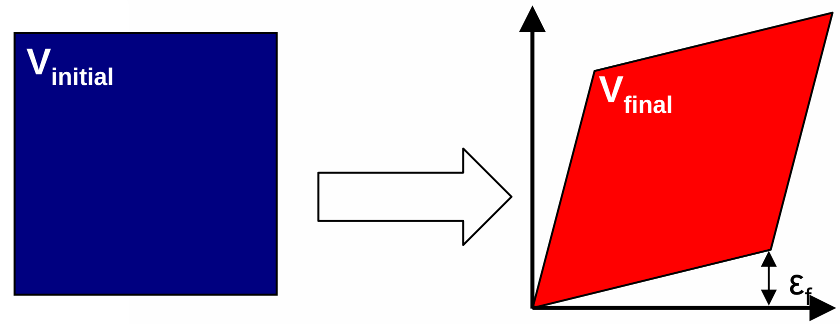

Prescribed average deformation

- Free-energy minimizers need not be uniform deformations (pure phases)
- Free energy can be reduced by mixing different phases (deformation patterning)

Goal: understand energy-minimizing deformation patterns (microstructures)

Microstructure of martensite

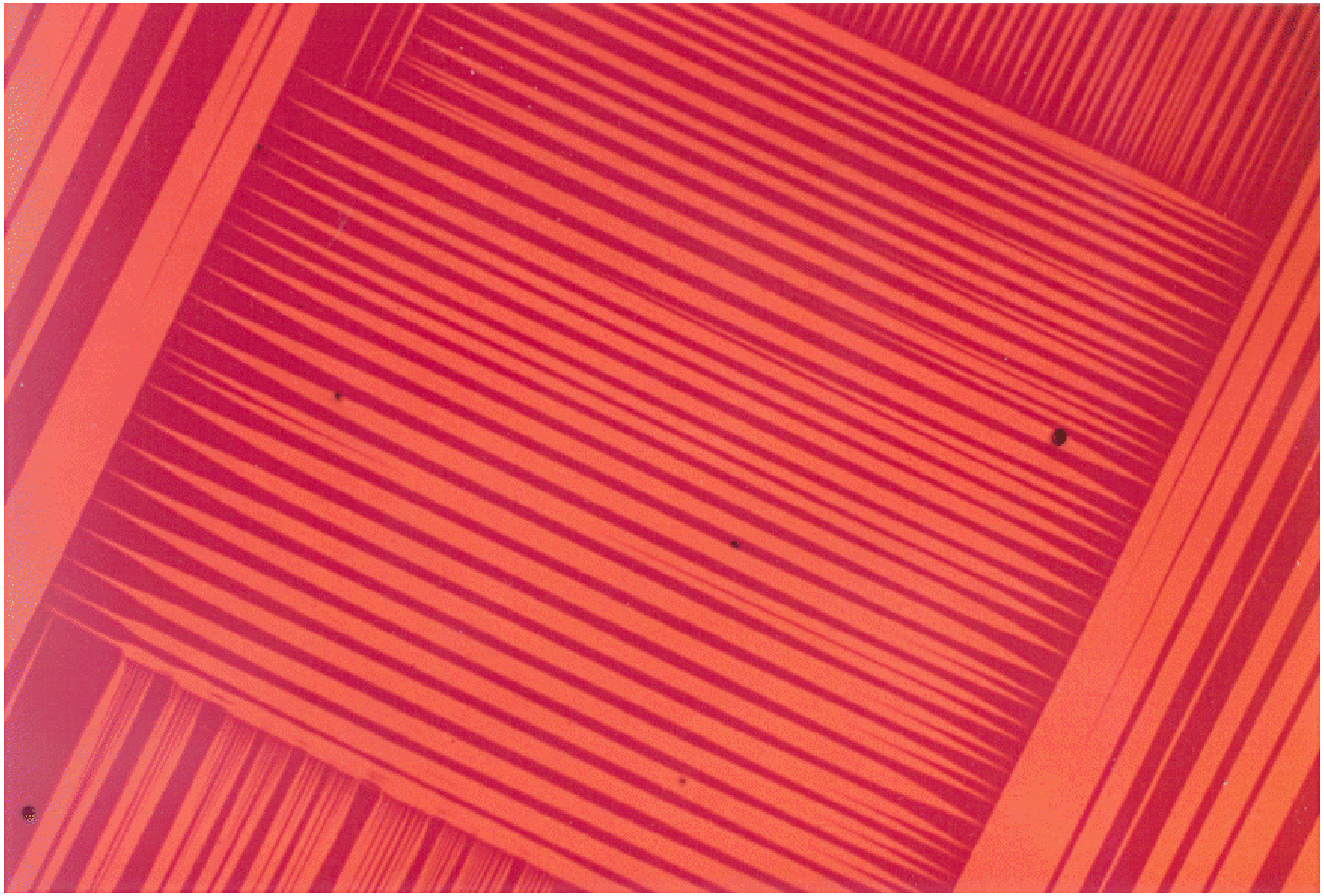

Cu-Al-Ni, Chunhua Chu and Richard D. James

Microstructure of martensite

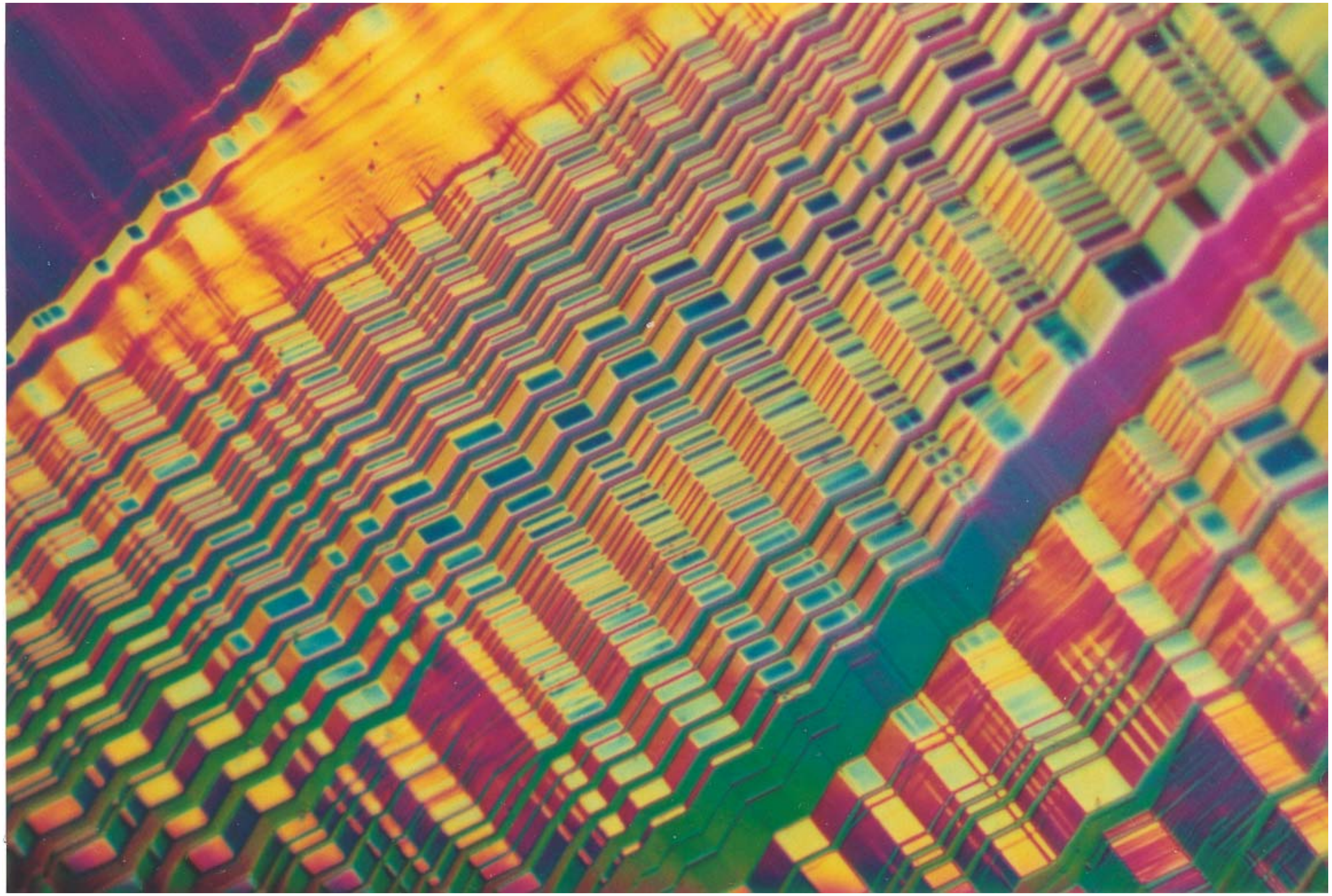

Cu-Al-Ni, Chunhua Chu and Richard D. James

Sequential laminates

Ansatz: Free-energy minimizing microstructures are sequential laminates

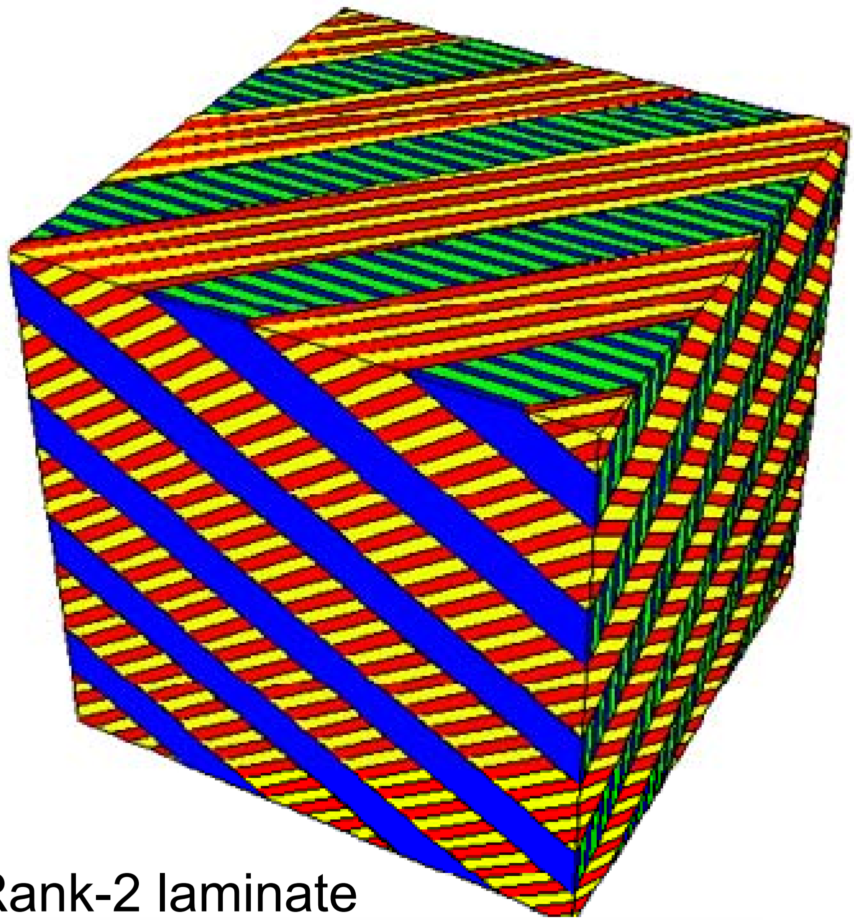

Rank-2 laminate

Simple laminate

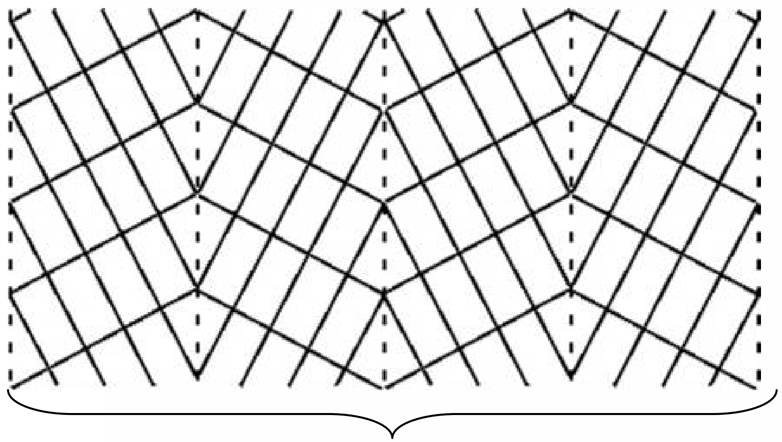

Coherent interfaces

- Must optimize:
  - Interfacial orientations
  - Volume fractions
  - Nesting of laminates
  - Variant sizes
- Constraints:
  - Equilibrium at interfaces
  - Coherent interfaces

(Aubry, Fago and Ortiz, *CMAME,* 2003)

Shear Compression

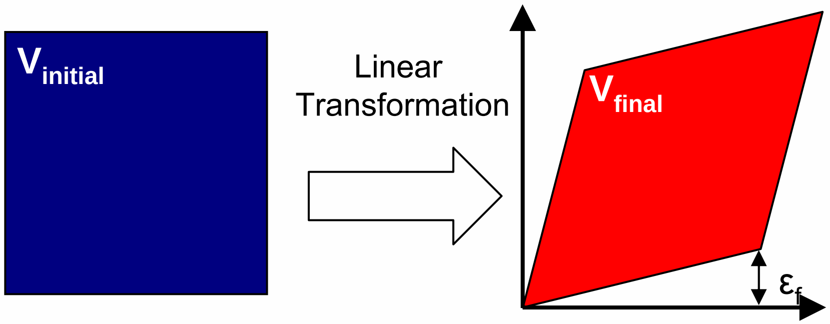

$$\boldsymbol{F}(\delta) = (1-\delta)\begin{pmatrix} 1 & 0 & 0 \\ 0 & 1 & 0 \\ 0 & 0 & 1 \end{pmatrix} + \delta\begin{pmatrix} \lambda & \varepsilon_f & 0 \\ \varepsilon_f & \lambda & 0 \\ 0 & 0 & \lambda \end{pmatrix}$$

undeformed *bcc*

λ is set such that $V=V_f$

(Note: det[***F***]=V)

$\varepsilon_f = 0.03$

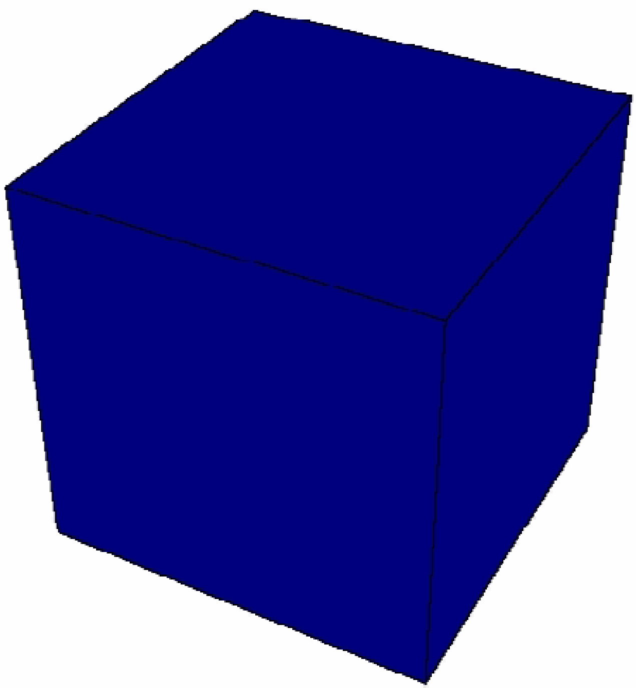

$\varepsilon_f = 0.04$

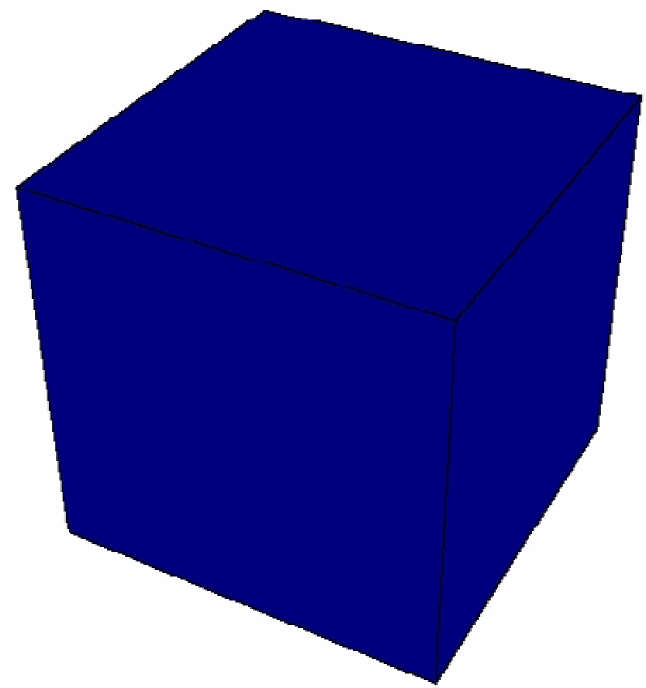

Note: mapped deformed volume onto reference volume

Role of Shear

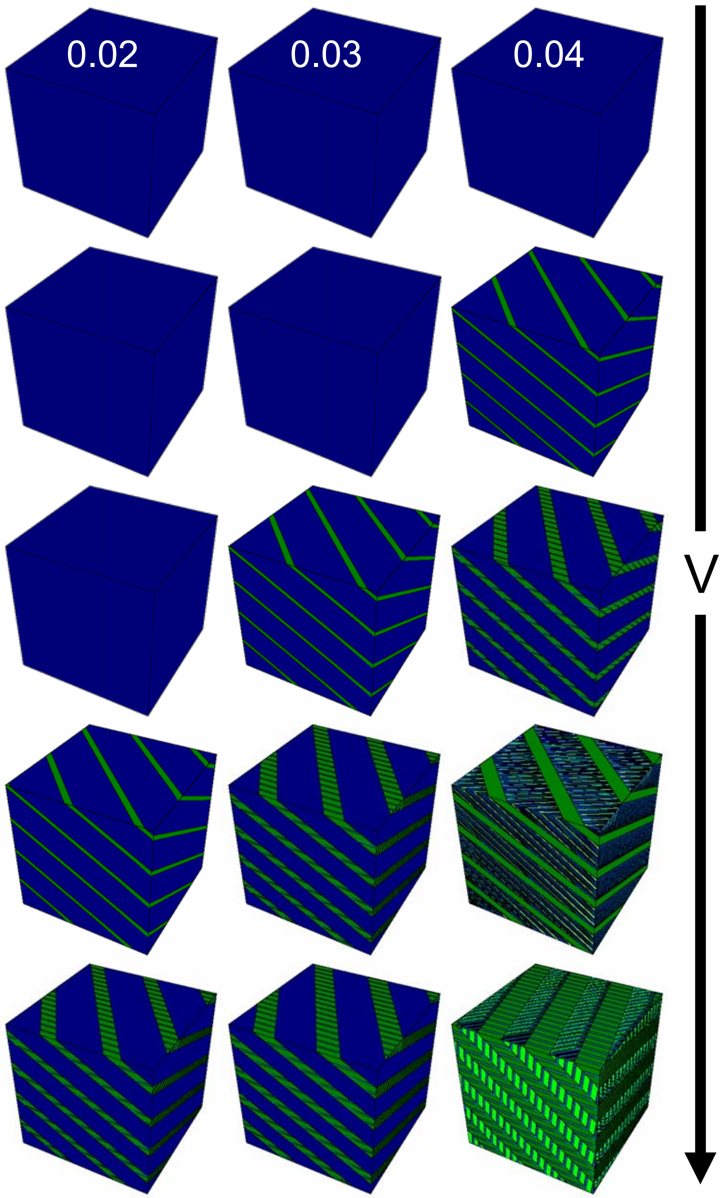

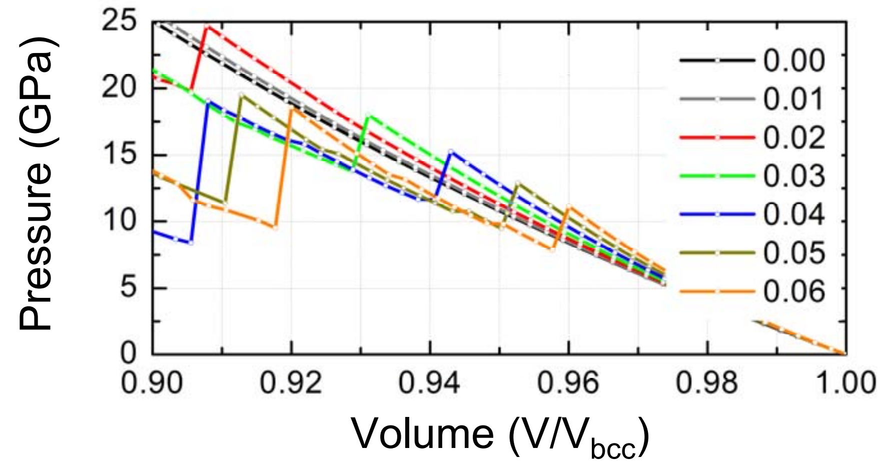

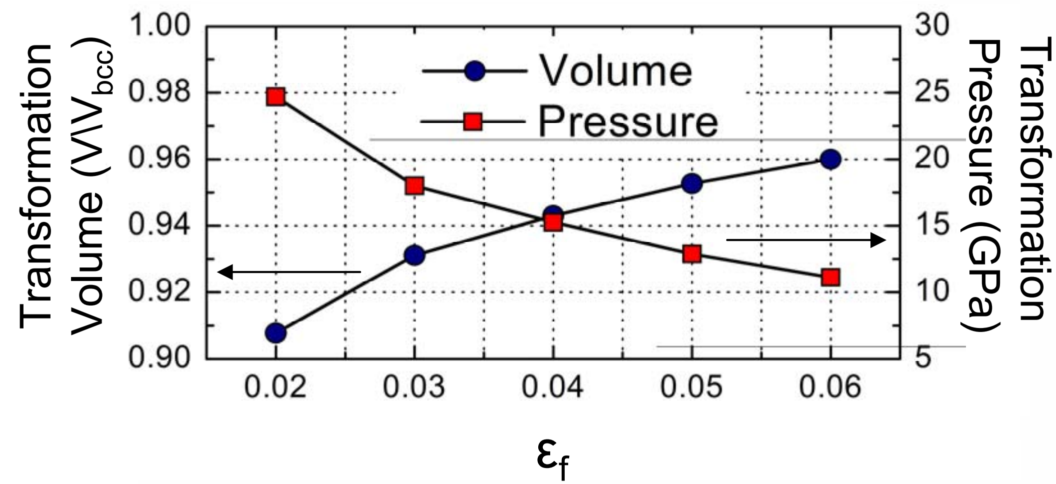

- shear is required to activate this transformation
- increasing shear lowers the TP and increases the TV
- variability in measured TPs may be due to shear states

bcc → *hcp* Phase Transformation

What are the average bulk properties of the bcc → hcp transformation?

To explore the transformation, we apply a series of volume-conserving deformations (F) along the transformation path.

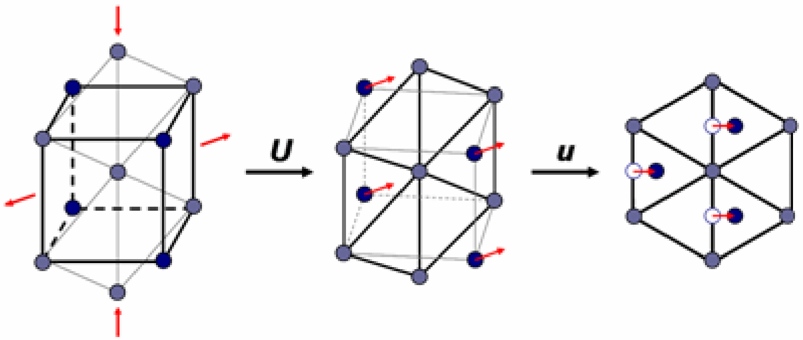

$$\boldsymbol{U}(V) = \begin{pmatrix} \frac{\alpha(V)}{2} + \frac{3}{4\sqrt{2}} & \frac{\alpha(V)}{2} - \frac{3}{4\sqrt{2}} & 0 \\ \frac{\alpha(V)}{2} - \frac{3}{4\sqrt{2}} & \frac{\alpha(V)}{2} + \frac{3}{4\sqrt{2}} & 0 \\ 0 & 0 & \frac{\sqrt{3}}{2} \end{pmatrix}$$

$$\alpha(V) = \sqrt{3/8}\,(c/a)_V$$

bcc **deformation**

$$\boldsymbol{F}_{bcc}(V) = V^{1/3}\,\boldsymbol{I}$$

hcp **deformation**

$$\boldsymbol{F}_{hcp}(V) = \left(\frac{V}{\det \boldsymbol{U}(V)}\right)^{1/3} \boldsymbol{U}(V)$$

linear transformation

$$\boldsymbol{F}(V,\delta) = \omega_\delta\left[(1-\delta)\boldsymbol{F}_{bcc}(V) + \delta\,\boldsymbol{F}_{hcp}(V)\right]$$

ω = volume-conserving scale factor

$0 \le \delta \le 1$

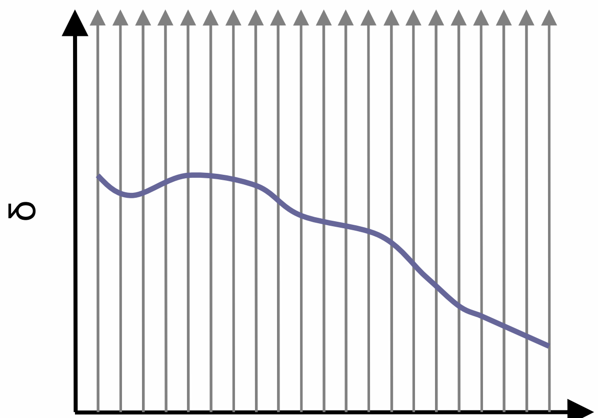

The F(V,δ) that minimizes W determines the transformation properties.

bcc → *hcp* Phase Transformation

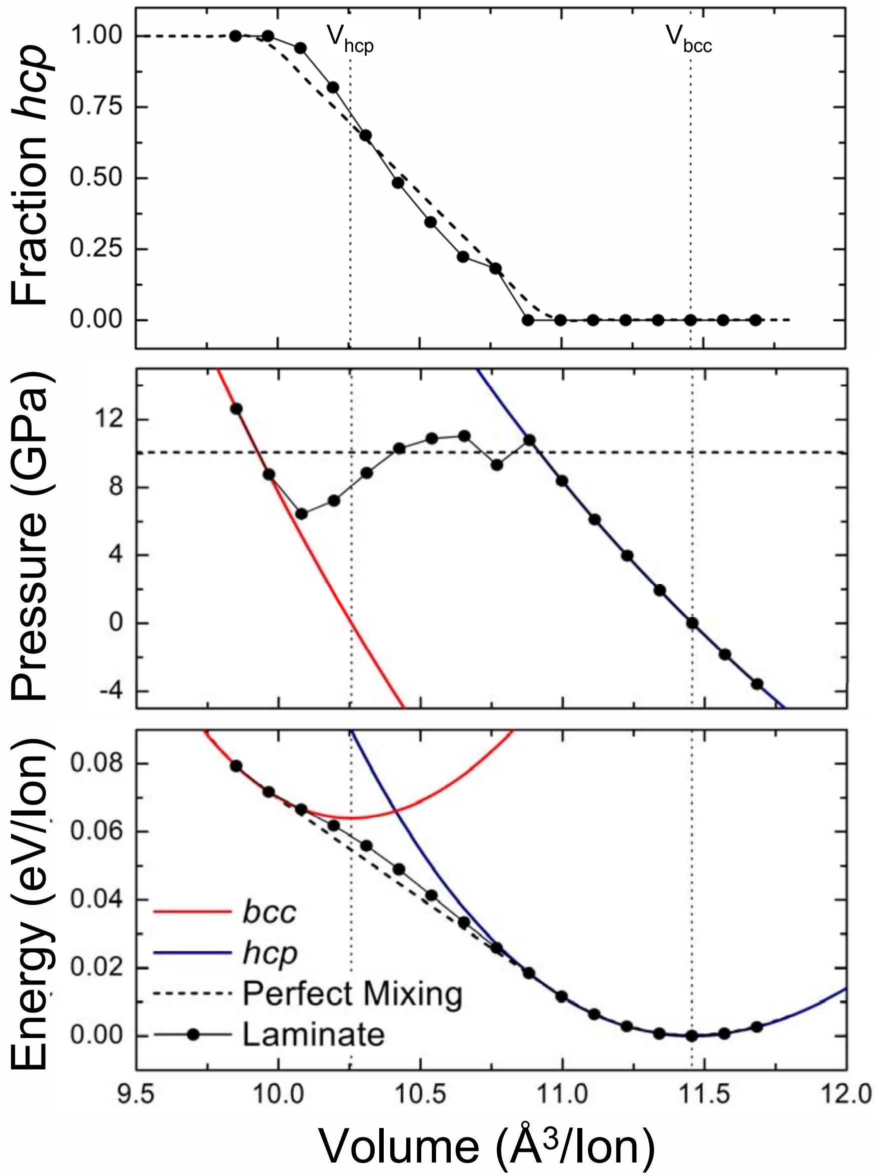

- **full conversion to *hcp***
- **transition pressure of 10 GPa**
- **hallmarks of Gibbs construction**
  - the lowering of the energy
  - the lag to full conversion to hcp
- **deviation from Gibbs construction**
  - no perfect tangent matching
  - energy is increased
  - caused by the two imposed constraints
    - Hadamard compatibility condition

$$\boldsymbol{F}_1 - \boldsymbol{F}_2 = \boldsymbol{a} \otimes \boldsymbol{n}$$

    - dependence on the transformation path

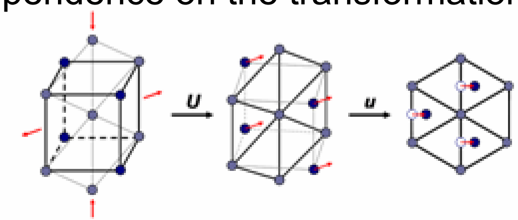

  - constraints introduce frustration
- **hysteresis width of ≈5.2 GPa observed**
  - loading TP = 10.2 GPa
  - unloading TP = 5.0 GPa
  - experimental width 6.2 GPa (Taylor et al.)

Directional Deformation of bcc Fe

- propagating shock waves apply load in specific directions

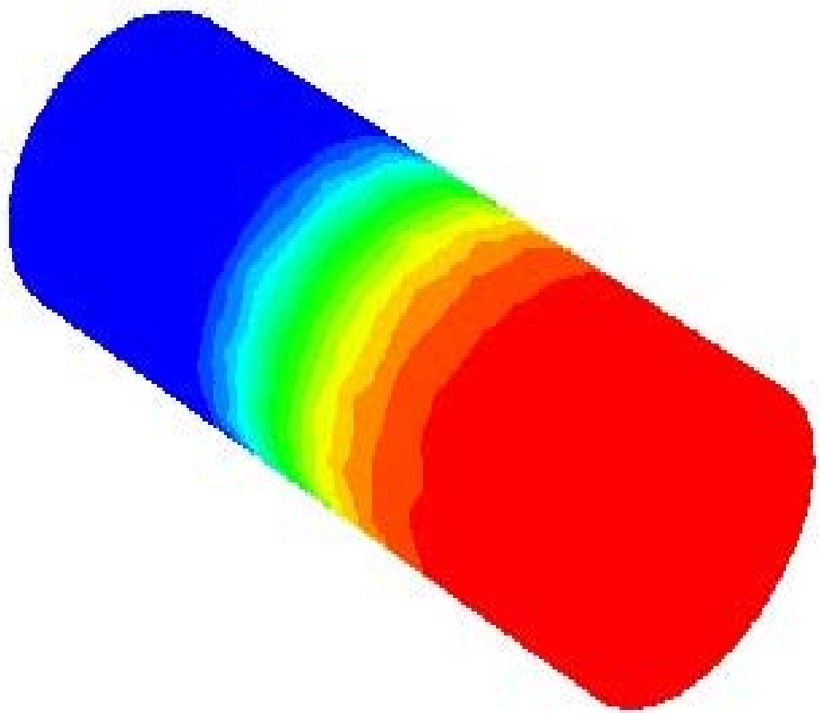

- what effect does the direction of applie load have on the transformation?

vestigate directional loading we applied lirectional deformation $F_{\theta,\varphi}(\delta)$ spanning rection space (angle space)

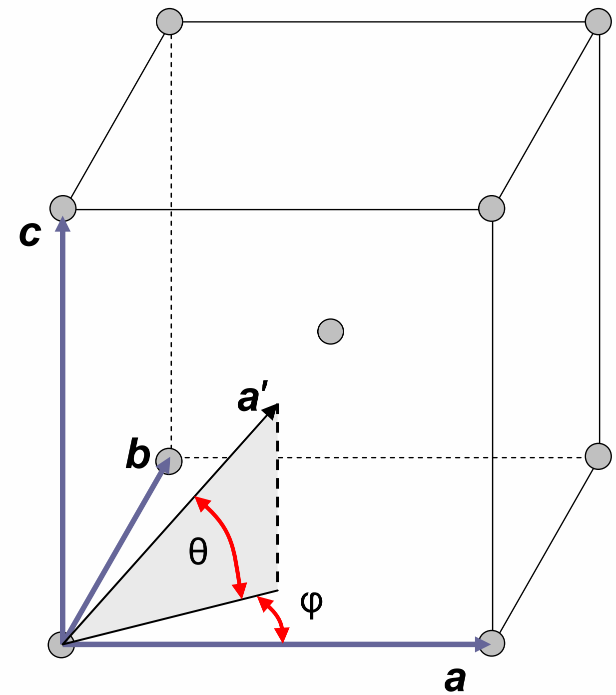

$$(\boldsymbol{a}',\boldsymbol{b}',\boldsymbol{c}') = \begin{pmatrix} \cos\varphi & \sin\varphi & 0 \\ -\sin\varphi & \cos\varphi & 0 \\ 0 & 0 & 1 \end{pmatrix} \begin{pmatrix} \cos\theta & 0 & \sin\theta \\ 0 & 1 & 0 \\ -\sin\theta & 0 & \cos\theta \end{pmatrix}$$

$$\boldsymbol{F}_{\theta,\varphi}(\delta) = \delta(\boldsymbol{a}' \otimes \boldsymbol{a}') + (\boldsymbol{b}' \otimes \boldsymbol{b}') + (\boldsymbol{c}' \otimes \boldsymbol{c}')$$

Directional Deformation of bcc Fe: TP and TV

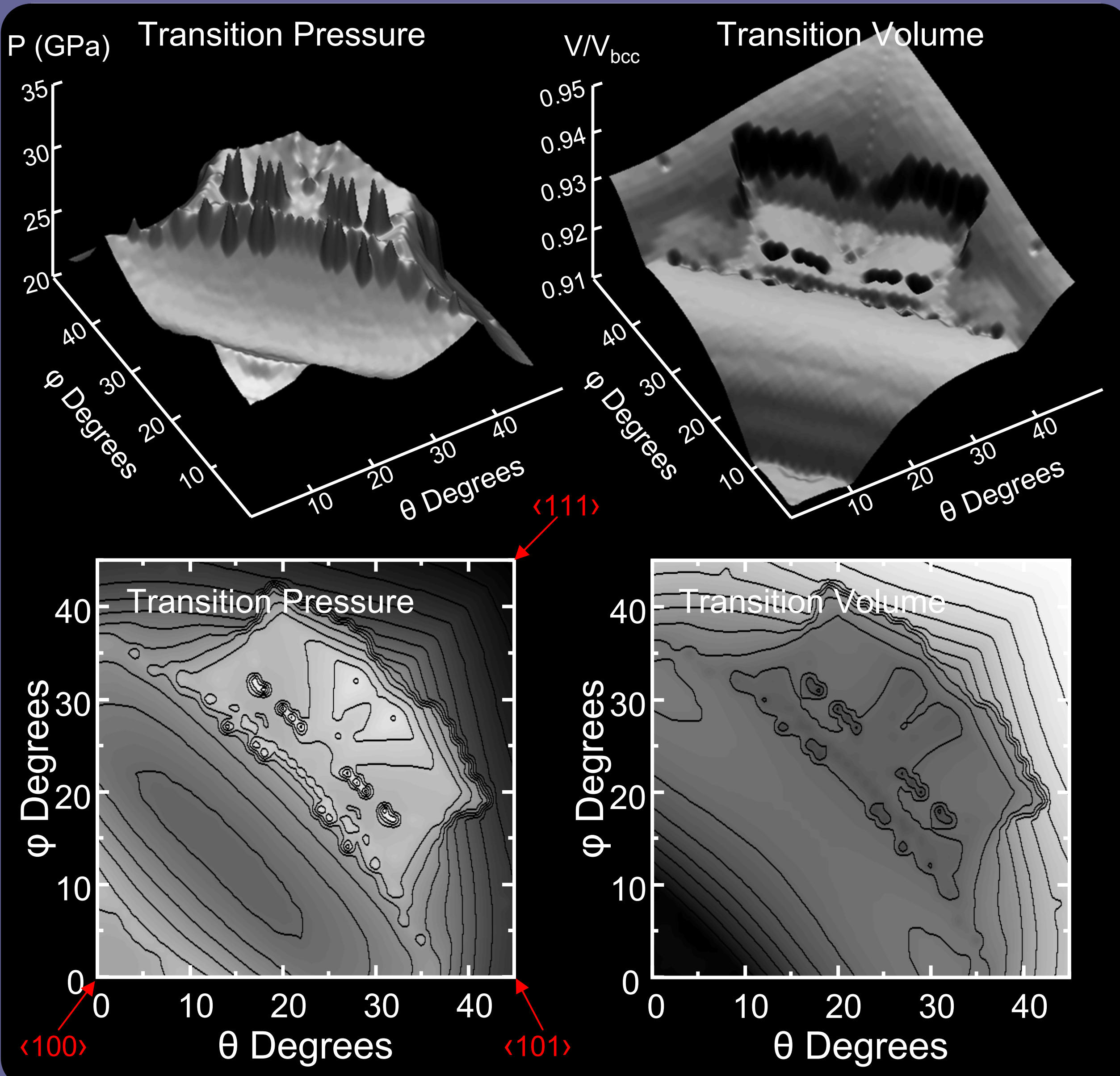

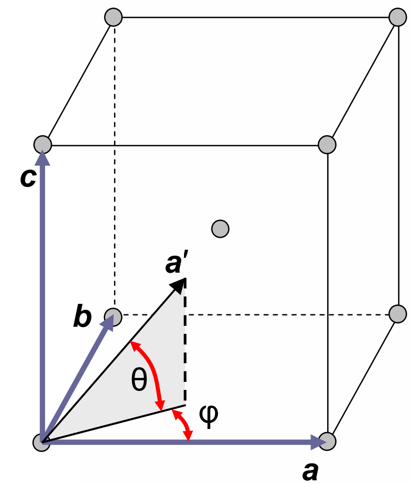

TP for all angles is high, >20 GPa

- never optimal combination of contraction and and shear

region of high pressure for moderate angles

- perhaps no hcp variant along path

loading parallel to simple facets facilitates the transformation

- notably the ‹110› planes

loading along the simple axes recovers smallest TP in that region of angle space

- ‹111›< ‹101›< ‹100›

First-principles input at finite temperature

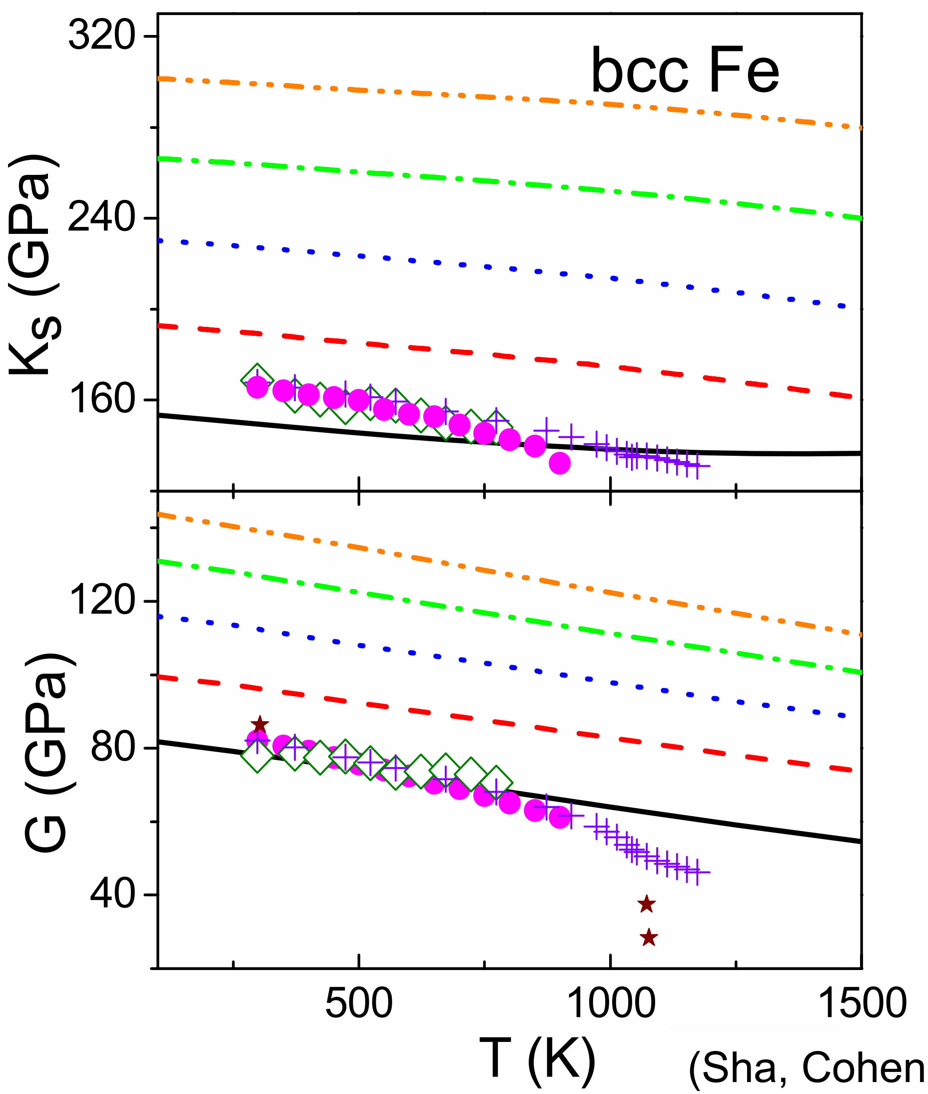

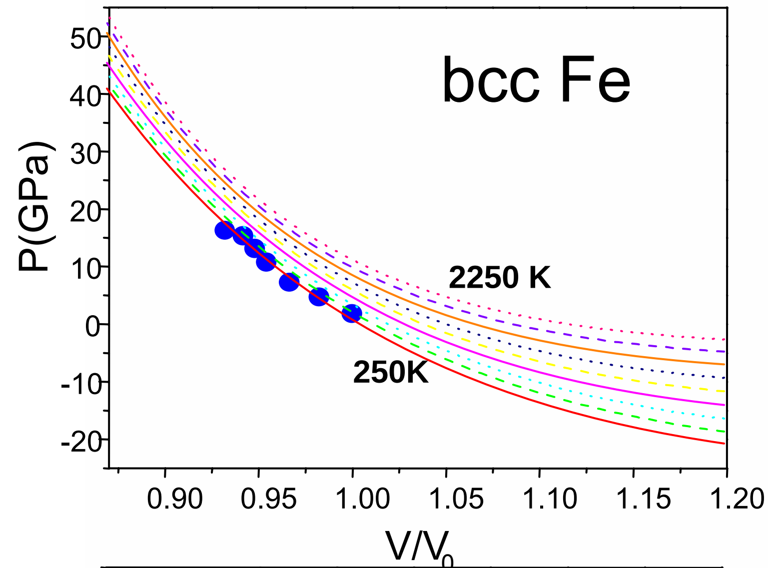

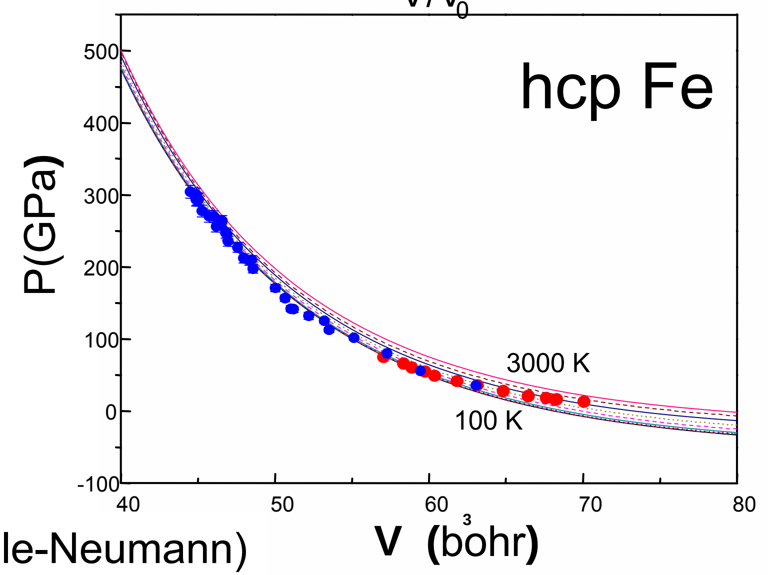

(Sha, Cohen, Steinle-Neumann)

Effect of temperature and plasticity

The pressure/volume properties of Fe subject to external strain at room temperature

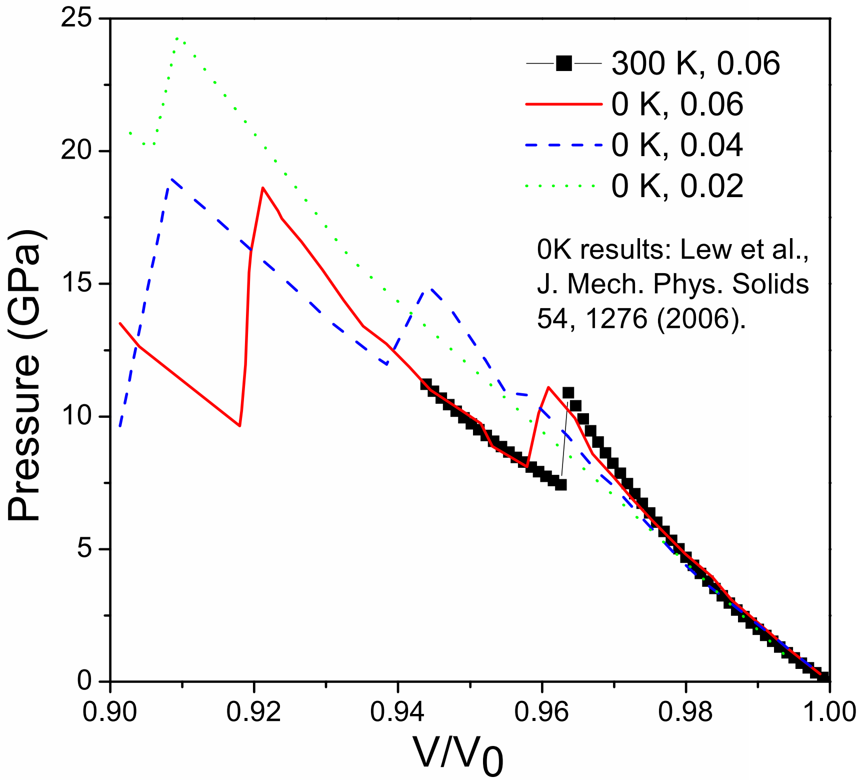

(Sha, Cohen, Steinle-Neumann)

Preliminary results show that the temperature effects are not very significant, but still the phase transformation tends to occur at lower pressures at room temperature than at zero temperature.

Plasticity also generates lamintes:

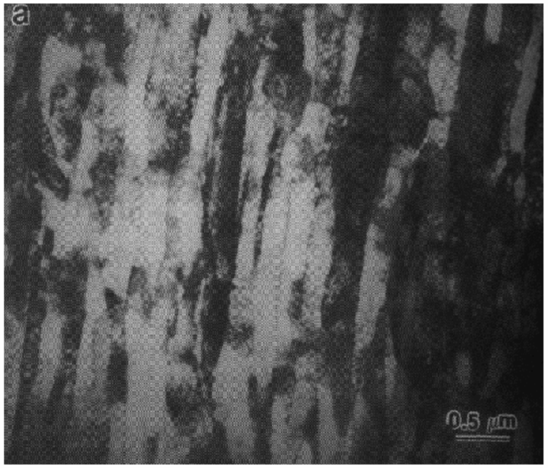

Shocked Ta (Meyers et al., 1995)

Conclusions

Shear Compression

- shear is required for transformation to occur
- increasing shear lowers the TP and increases the TV
- sensitivity to shear may be responsible for the variability in the measured TPs

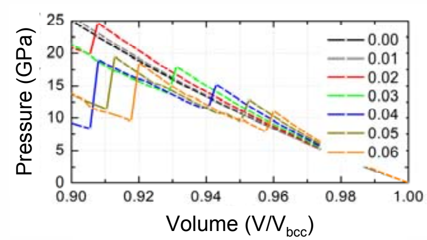

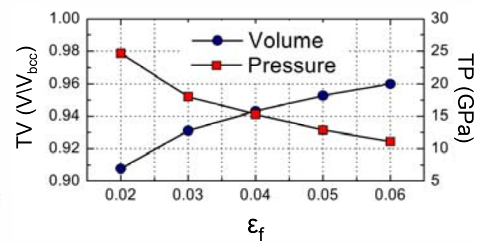

bcc-to-hcp Transformation

- full conversion to *hcp at* ≈10 GPa*,* consistent with the experimentally observed values
- hallmarks of the Gibbs construction
- deviation from "perfect" mixing due to imposed constraints
- shows hysteresis in the TP simply due to the crystalline kinematics

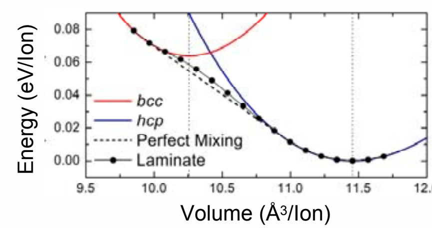

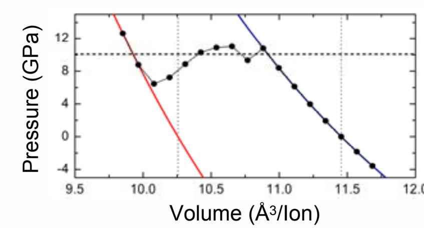

$$F_1 - F_2 = a \otimes n$$

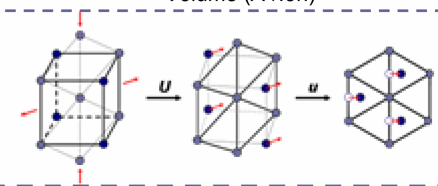

Directional Deformation

- transformation pressure is > 20GPa
- region of very high transformation pressure
- loading || to simple facets facilitates the transformation, in particular along simple axes

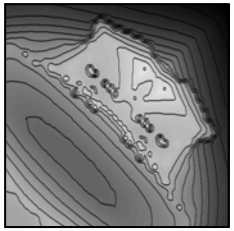

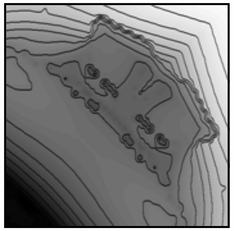

Acknowledgements

Matt Fago :S. Aubry, M. Fago, and M. Ortiz, Computer Methods in Applied Mechanics and Engineering **192**, 2823 (2003).

De-en Jiang Robin Hayes Emily Jarvis , Sha, Cohen, Steinle-Neumann